

Development of cerebral fiber pathways in cats revealed by diffusion spectrum imaging

Emi Takahashi^{a,b,c,*}, Guangping Dai^{a,b}, Ruopeng Wang^b, Kenichi Ohki^d, Glenn D. Rosen^e, Albert M. Galaburda^e, P. Ellen Grant^{a,b,c,f,1}, Van J. Wedeen^{a,b,1}

^a Department of Radiology, Harvard Medical School, Charlestown, MA, USA

^b A. A. Martinos Center for Biomedical Imaging, Massachusetts General Hospital, Charlestown, MA, USA

^c Department of Medicine, Division of Newborn Medicine, Children's Hospital Boston, Harvard Medical School, Boston, MA, USA

^d Department of Neurobiology, Harvard Medical School, Boston, MA, USA

^e Department of Neurology, Beth Israel Deaconess Medical Center, Harvard Medical School, Boston, MA, USA

^f Department of Radiology, Children's Hospital Boston, Harvard Medical School, Boston, MA, USA

ARTICLE INFO

Article history:

Received 6 May 2009

Revised 23 August 2009

Accepted 1 September 2009

Available online 8 September 2009

Keywords:

Diffusion Spectrum Imaging

Tractography

Development

Thalamo-cortical tracts

Cat

ABSTRACT

Examination of the three-dimensional axonal pathways in the developing brain is key to understanding the formation of cerebral connectivity. By tracing fiber pathways throughout the entire brain, diffusion tractography provides information that cannot be achieved by conventional anatomical MR imaging or histology. However, standard diffusion tractography (based on diffusion tensor imaging, or DTI) tends to terminate in brain areas with low water diffusivity, indexed by low diffusion fractional anisotropy (FA), which can be caused by crossing fibers as well as fibers with less myelin. For this reason, DTI tractography is not effective for delineating the structural changes that occur in the developing brain, where the process of myelination is incomplete, and where crossing fibers exist in greater numbers than in the adult brain. Unlike DTI, diffusion spectrum imaging (DSI) can define multiple directions of water diffusivity; as such, diffusion tractography based on DSI provides marked flexibility for delineation of fiber tracts in areas where the fiber architecture is complex and multidirectional, even in areas of low FA. In this study, we showed that FA values were lower in the white matter of newborn (postnatal day 0; P0) cat brains than in the white matter of infant (P35) and juvenile (P100) cat brains. These results correlated well with histological myelin stains of the white matter: the newborn kitten brain has much less myelin than that found in cat brains at later stages of development. Using DSI tractography, we successfully identified structural changes in thalamo-cortical and cortico-cortical association tracts in cat brains from one stage of development to another. In newborns, the main body of the thalamo-cortical tract was smooth, and fibers branching from it were almost straight, while the main body became more complex and branching fibers became curved reflecting gyrification in the older cats. Cortico-cortical tracts in the temporal lobe were smooth in newborns, and they formed a sharper angle in the later stages of development. The cingulum bundle and superior longitudinal fasciculus became more visible with time. Within the first month after birth, structural changes occurred in these tracts that coincided with the formation of the gyri. These results show that DSI tractography has the potential for mapping morphological changes in low FA areas associated with growth and development. The technique may also be applicable to the study of other forms of brain plasticity, including future studies *in vivo*.

© 2009 Elsevier Inc. All rights reserved.

Introduction

Among the essential defining features of the immature brain, compared to the adult brain, are its dynamically developing fiber circuitry and progressive myelination. Major events in the development of cerebral connections include the growth of thalamo-cortical axons into the cortical plate (CP), which later develops into the adult

cortex, and the formation of thalamo-cortical synaptic connections in the CP. The latter initiates the permanent, sensory-driven circuitry established around prenatal week (W) 24 in humans (Kostovic and Jovanov-Milosevic, 2006) and around embryonic day (E) 50 in cats (Hermann et al., 1994; Johnson and Casagrande, 1993). Following the formation of the thalamo-cortical tracts, other major afferent fibers, such as the basal-forebrain and cortico-cortical association fibers, also grow and accumulate below the CP. Coincident with the formation of these fiber pathways is the process of axonal myelination, which starts well before birth in humans and continues, depending on location in the brain, until adulthood (Yakovlev and Lecours, 1967; Brody et al., 1987).

* Corresponding author. Department of Medicine, Division of Newborn Medicine, Children's Hospital Boston, Harvard Medical School, Boston, MA, USA.

E-mail address: emi@nmr.mgh.harvard.edu (E. Takahashi).

¹ These authors equally contributed to this work as senior authors.

During the late fetal period and early preterm period, the most prominent transient layer is the subplate (SP) zone, which contains waiting thalamo-cortical afferent fibers crossing one another (Kostovic and Rakic, 1990; Allendoerfer and Shatz, 1994; O'Leary et al., 1994; Ulfing et al., 2000), and is involved in endogenous activity (for reviews, Allendoerfer and Shatz, 1994; Kostovic and Jovanov-Milosevic, 2006). The SP develops around prenatal week (W) 13 and gradually disappears after W 32–34 in humans (Kostovic and Rakic, 1990; Ulfing et al., 2000), which corresponds to embryonic day (E) 25 through postnatal day (P) 60 in cats (Allendoerfer and Shatz, 1994; O'Leary et al., 1994; Issa et al., 1999).

There have been many detailed tracer studies of the axonal connections, and also many conventional MRI studies of the white matter, in developing brains. However these conventional methods are associated with three major technical limitations (Mori, 2007). First, because the white matter appears homogenous in images acquired with conventional MRI, it is difficult to appreciate fiber pathways in the white matter. Second, approaches employing tracer injections can study only a small number of white matter tracts in a given brain and cannot be used for global anatomical characterization, nor can they be used sequentially in the same subject to follow development or the effect of an experiment. Third, and most importantly, invasive approaches cannot be used in living human beings. By virtue of the recent technical advances in diffusion-weighted magnetic resonance imaging (DWI), we can now study global white matter neuronal fiber connections (Basser et al., 1994, 2000; Pierpaoli et al., 1996; Cellierini et al., 1997; Makris et al., 1997; Mori et al., 1999; Jones et al., 1999; Conturo et al., 1999; Le Bihan et al., 2001; Catani et al., 2002; Takahashi et al., 2007, 2008; Hagmann et al., 2008).

DWI is based on measurement of the restricted diffusion of water molecules in brain tissue (Basser et al., 1994). DWI and associated analyses, which assume that water diffusivity is represented by an ellipsoid tensor in each voxel, are referred to as diffusion tensor imaging (DTI). The use of algorithms to reconstruct 3D axonal white matter trajectories from DWI data (Mori et al., 1999; Jones et al., 1999; Conturo et al., 1999) is often referred to as diffusion tractography, and tractography that takes into account the directions of maximum water diffusivity represented by ellipsoid tensors is specifically called DTI tractography. Diffusion tractography permits examination (1) of white matter axonal connections running in many directions, (2) throughout the entire brain, and (3) *in vivo*; such examination is not achieved using conventional techniques. Conventional MRI techniques have indeed demonstrated developmental myelination processes (Barkovich et al., 1988; Van der Knaap and Valk, 1990; for review Paus et al., 2001), but DWI and DTI provide greater sensitivity for visualizing the maturation of white matter fibers (Rutherford et al., 1991; Sakuma et al., 1991; Huppi et al., 1998; Neil et al., 1998; Baratti et al., 1999; for review Neil et al., 2002).

Diffusion fractional anisotropy (FA), one of the indices derived from DWI, represents the directional bias of water diffusivity in each image voxel, that is, the preferred direction of diffusion, which may be dictated by a structural bias such as the direction taken by a bundle of white matter fibers. Low diffusion anisotropy (low FA) corresponds to low directional bias of water diffusivity, and thus a low underlying preferential orientation of fibers, or a mix of fibers traveling in several directions (such as crossing fibers). The effect of FA on conventional diffusion tractography depends largely on two determining factors: (1) the tensor model, which can drive tractography in the wrong direction in areas of low FA, and (2) the FA threshold, which is typically set to terminate tractography-derived fibers in areas with low FA values; i.e., in areas where the FA values measured are below the threshold. Although the nonmyelinated central nervous systems such as olfactory nerves (Beaulieu and Allen, 1994) and white matter of premature newborns (Huppi et al., 1998) and young animals feature some degree of diffusion anisotropy (Wimberger et al., 1995; Prayer et al., 2001), FA remains low wherever fibers cross and/or are

less myelinated. As such, these are two major concerns relevant to the use of conventional DTI tractography for studies of the neonatal brain; we describe them in greater detail in the following sections.

First, a single voxel can contain more than one fiber orientation, such as when multiple fibers cross one another within a voxel. It is known that many complex crossing pathways arrive during development under the CP at the subplate zone known as the subplate (SP) (Kostovic and Rakic, 1990; Allendoerfer and Shatz, 1994; O'Leary et al., 1994; Ulfing et al., 2000). During the late fetal period/early preterm period, the SP is the most prominent transient layer, and it plays a crucial role in aiding immature axons in finding their destinations in the CP. It is not an area that can be overlooked if one is to understand the development of cortical connectivity. Second, the immature brain is less myelinated than the adult brain, which leads to lower overall FA values in white matter. Nonetheless, some studies have reported FA changes in the developing brain structures of mice (e.g. Zhang et al., 2003) and humans (McKinstry et al., 2002; Partridge et al., 2004; Maas et al., 2004), and other studies have recently tracked 3D fiber pathways in neonatal human brains (e.g. Zhai et al., 2003; Yoo et al., 2005; Dubois et al., 2006). However, structural changes in white matter bundles in developing brains have not been accurately explored for the reasons above.

In contrast to diffusion tensor imaging, diffusion spectrum imaging (DSI) models water diffusion in each MR voxel by measuring both the orientation distribution function (ODF) and the diffusion spectrum, i.e., the full probability distribution of the diffusion of water molecules (Wedeen et al., 2005). By virtue of its ability to define multiple directions of water diffusivity along crossing fibers, DSI provides flexibility that permits delineation of fiber tracts in areas where the fiber architecture is complex and multidirectional. Compared to other forms of diffusion imaging, DSI is the most general (essentially model-free) approach (Wedeen et al., 2005), and recent studies have illustrated its effectiveness for imaging complex white matter structure (Schmahmann et al., 2007; Wedeen et al., 2008). Motivated by the challenges of conventional diffusion tractography, we used a DSI tractography approach (that did not use FA values to terminate tractography; see below for method used to end tracking here) to accurately depict the developing thalamo-cortical tracts that pass areas of crossing fibers in newborn kittens, including areas with less myelination.

We examined *ex vivo* cat brains. *Ex vivo* imaging provides the benefit of very high resolution and high signal-to-noise-ratio at the cost of very long image acquisition sessions, which, however, are not practical *in vivo*. There were three reasons behind our choice of the cat brain for these investigations: (a) *ex vivo* human fetal brains are not easily obtained, (b) the size of the cat brain lends itself to examination with small bore MR systems (4.7T and 9.4T) capable of producing high-resolution signals, which can be then compared to histological results, and (c) adult cat brains have relatively complex gyral folding patterns, and therefore provide closer comparison to monkeys and humans than do the brains of rats and mice.

Increasing numbers of diffusion studies on developing animal (Zhang et al., 2003, 2005; Huang et al., 2006; Kroenke et al., 2007; Huang et al., 2008; D'Arceuil et al., 2008; Kuo et al., 2008), fetal and newborn human brains (Rutherford et al., 1991; Sakuma et al., 1991; Huppi et al., 1998; Neil et al., 1998; Baratti et al., 1999; for review Neil et al., 2002; Prayer et al., 2006; Rollins, 2007; Huang et al., 2009) have reported that FA values increase in the white matter with age. Some investigators have also performed diffusion tractography in animals (Zhang et al., 2003; Kim et al., 2003; D'Arceuil et al., 2008) and humans (Berman et al., 2005; Bui et al., 2006; Huang et al., 2006; Bassi et al., 2008; Kasprian et al., 2008; Huang et al., 2009) showing the development of major white matter pathways. However, these studies did not illustrate the entire lengths of the cerebral connections extending into the gray matter (or the cortical plate), probably because of the existence of low FA areas, crossing fibers and regions

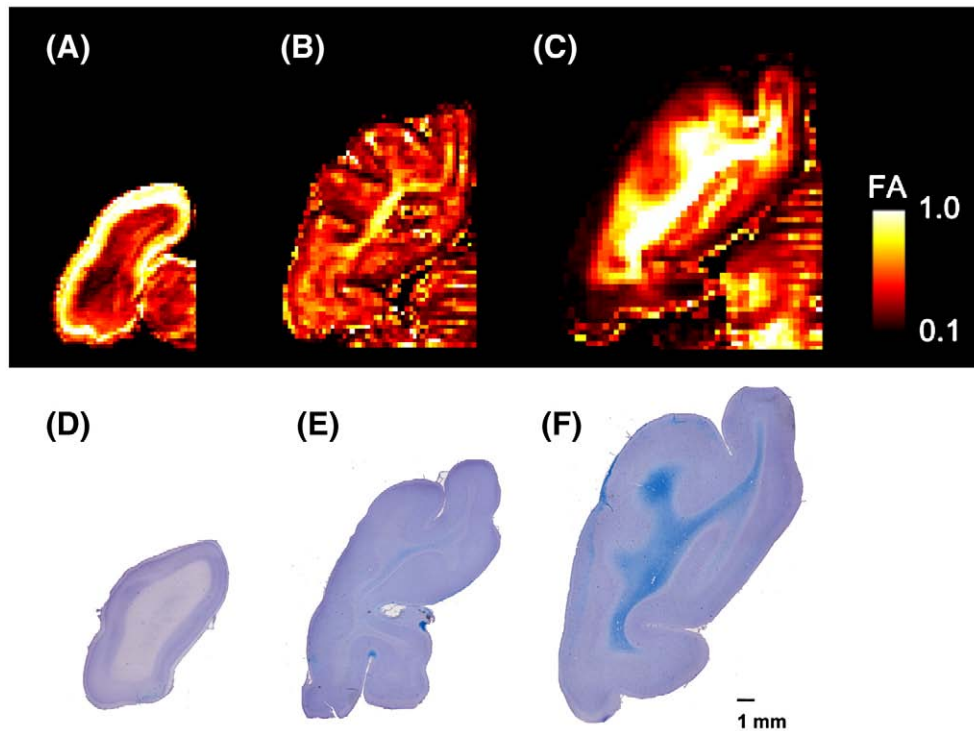


Fig. 1. (A–C) FA maps of individual cat brains (left hemisphere) at ages P0 (A), P35 (B) and P100 (C). The color scale indicates FA values. The left side of the image represents the left side of the brain. (D–F) Luxol fast blue stains counterstained by cresyl violet for P0 (D), P35 (E), and P100 (F) brain sections. Luxol fast blue stain reveals myelin (in blue), and cresyl violet, the cell bodies (in violet). The scale bar indicates 1 mm.

where fibers take a sharp turn (almost 90 degrees) as they enter the cortex. All of these factors can result in termination of the fiber tracking. *In vivo* fetal tractography studies are currently limited to a minimal number of gradient encoding directions and DTI reconstruction due to fetal motion, which severely limits scan times. Even post-natal infant studies are limited due to motion artifacts. Typically, more diffusion encoding directions are used in infants, but time limitations necessitate DTI (Huang et al., 2006; Dubois et al., 2006, 2008a,b) or, at best, HARDI reconstructions, as the minimum DSI scan time is currently 20 min. 3T imaging with 32-channel coils has improved diffusion imaging quality and facilitated acquisition of 30-direction data, but 7T human diffusion studies currently suffer from the field inhomogeneities and are inferior to current 3T data. However, strategies for shortening DSI scan times are being actively pursued, and therefore, there is hope that feasible DSI sequences for infants will be possible in the near future.

Methods

Specimens

We examined the brains of two newborn kittens (postnatal day 0; P0), two infant kittens (P35), and two juvenile cats (P70 and P100), obtained from a laboratory involved in visual research. All procedures were approved by the Harvard Medical School. After the cats were euthanized, their brains were perfused with phosphate-buffered saline (PBS) solution followed by 4% paraformaldehyde, removed from the cranium, and fixed for 1 week in 4% paraformaldehyde solution containing 1 mM gadolinium (Gd-DTPA) MRI contrast agent to reduce the T_1 relaxation time while ensuring that enough T_2 -weighted signal remained. For MR image acquisition, the brains were placed in Fomblin. We used two Bruker Biospec MR systems: a 4.7-T scanner for all specimens and a 9.4-T system for the two neonate specimens.

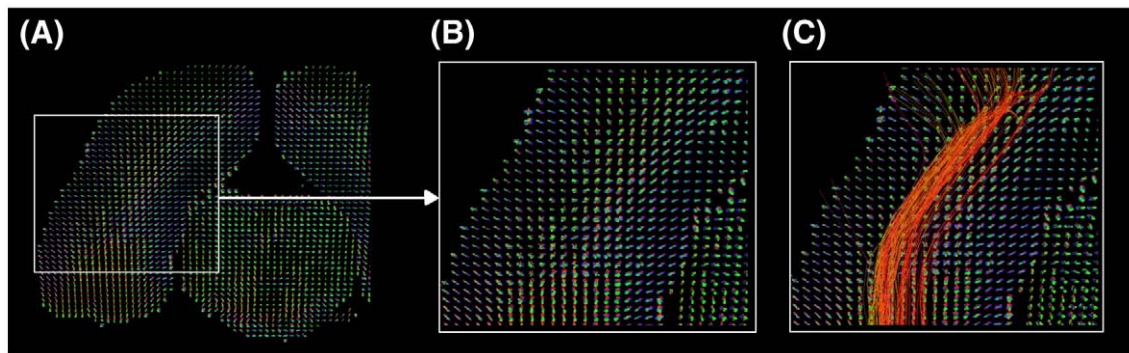


Fig. 2. Orientation distribution functions (ODFs) in the P0 brain. (A) ODFs corresponding to the visual areas shown in Fig. 1. (B) Magnified image of the region shown within the rectangle in (A). (C) Tractography fibers overlaid on the ODFs. The left side of the image represents the left side of the brain. The color-coding of the ODFs is based on standard RGB code, applied to the orientation vectors.

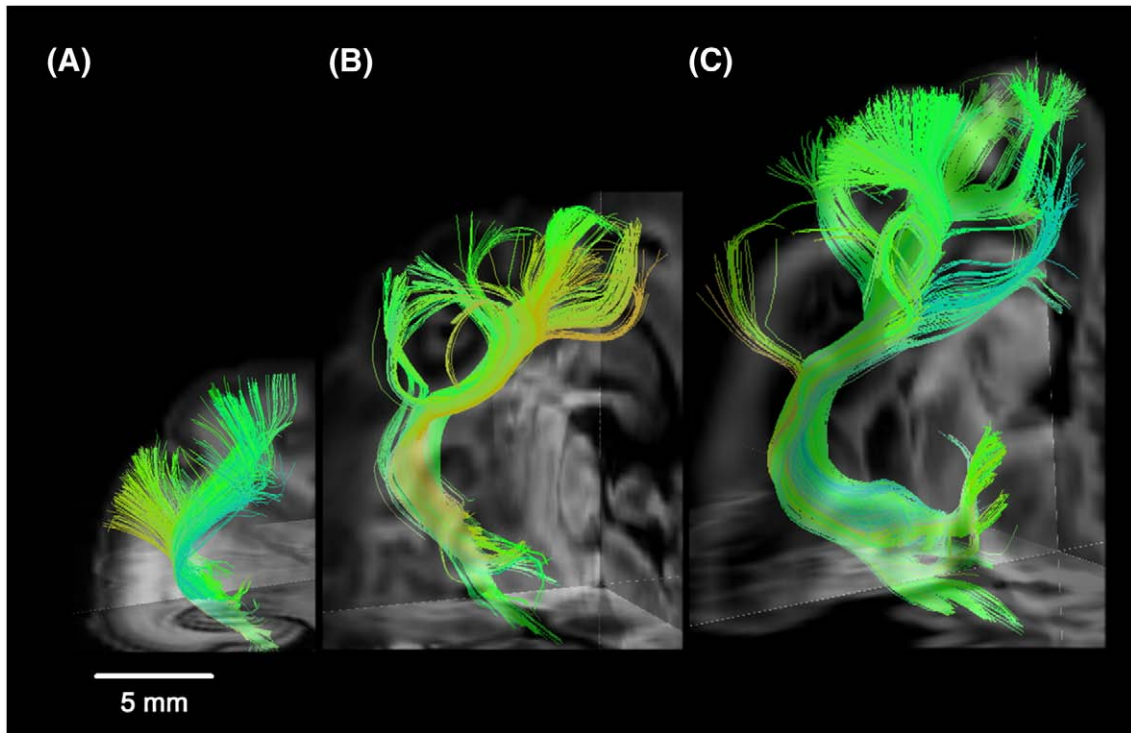


Fig. 3. 3D views of the thalamo-cortical tracts between the lateral geniculate nucleus and the primary visual cortex in all ages in P0 (A), P35 (B), and P100 (C) brains. The left side of the image represents the left side of the brain.

The presented images/data in each age group were from a single brain. The main reason why we only showed the data from a single brain was that it was difficult to get the two specimens of newborn kittens, and one of them was not in an optimal condition probably because it died for some reason before we perfused it.

Scanning parameters

The pulse sequence used for image acquisition was a 3D diffusion-weighted spin-echo echo-planar imaging (EPI) sequence, TR/TE 1000/40 ms, with an imaging matrix of $112 \times 112 \times 128$ pixels for P0 brains, $96 \times 112 \times 128$ pixels for P35 brains, and $96 \times 96 \times 128$ pixels for P70 and P100 brains. Spatial resolution was $300 \times 300 \times 300 \mu\text{m}$ for the newborn kittens, $420 \times 420 \times 420 \mu\text{m}$ for the juvenile kittens, and $550 \times 550 \times 600 \mu\text{m}$ for the young adult cats. Anisotropic resolution may produce less spatial resolution along a longer axis compared to that along a shorter axis, which may mean that DSI tractography has less potential to resolve crossing pathways in the direction along the

longer axis. However, the voxel size used for the young adult cats was nearly isotropic (less than 10% difference) and we believe it did not bias our tractography significantly.

We performed diffusion spectrum encoding as previously described (Wedeen et al., 2005). Briefly, we acquired 515 diffusion-weighted measurements, corresponding to a cubic lattice in q -space contained within the interior of a ball of maximum radius $b_{\text{max}} = 4 \times 10^4 \text{ cm}^2 \text{ s}^{-1}$, with $\delta = 12.0 \text{ ms}$, $\Delta = 24.2 \text{ ms}$. The total acquisition time was 18.5 h for each experiment.

Diffusion data analyses—DSI reconstruction

DSI reconstruction was based on the Fourier relationship of the attenuated echo signal in q -space $E(q)$ and the average diffusion propagator of the water molecular diffusion $P_s(R)$:

$$E(q) = \int P_s(R, \Delta) \exp(i2\pi qR) dR,$$

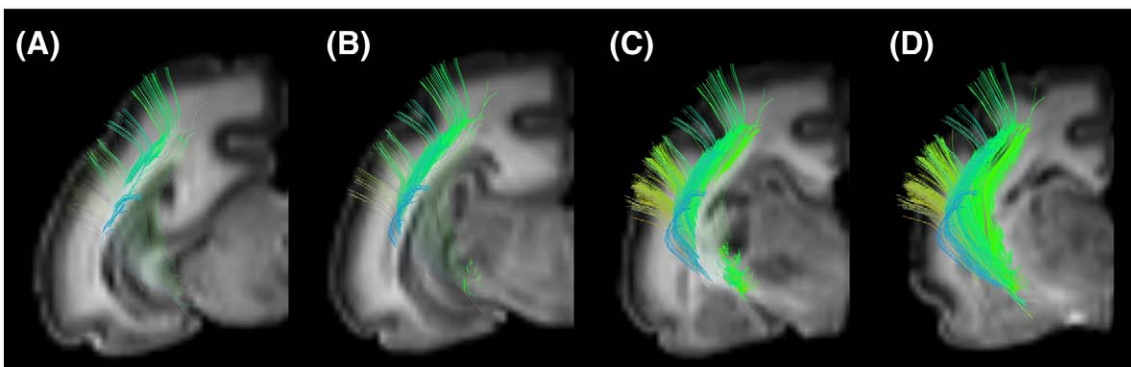


Fig. 4. Sequential coronal views of the thalamo-cortical tracts superimposed on DWIs, from posterior (A) to anterior (D).

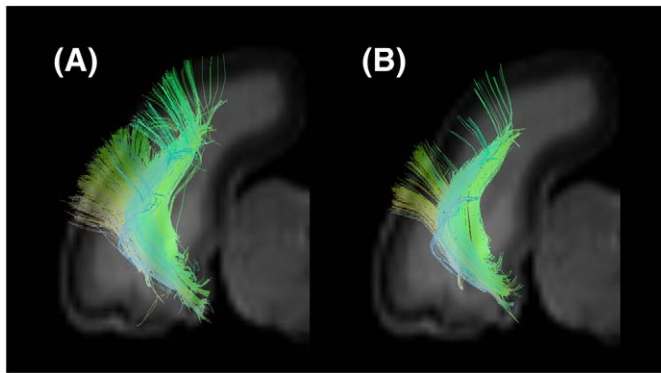


Fig. 5. Tractography on the thalamo-cortical tracts in the newborn kitten using a brain mask (A) and using conventional cut off FA values along with the brain mask (B).

where R is the relative displacement of water molecular diffusion during the diffusion time Δ (Callaghan, 1991). Based on this calculation, applying a 3-dimensional (3D) Fourier transform to the echo signal over the q -space would lead us to obtain the 3D probability density function (PDF) and then map the fiber orientations (Lin et al., 2003; Wedeen et al., 2005). The transformation from q -space signal to PDF values was performed voxel-by-voxel. To visualize the PDF, we integrated the second moment of PDF along each radial direction to acquire the orientation distribution function (ODF). In this study, we reconstructed the ODF within each voxel by interpolating along 181 radial directions, as calculated from the vertices of a regular and triangular mesh of the unit sphere surface. By comparing the length of each vector with the lengths of its neighboring vectors, we could obtain the orientational local maxima to represent intravoxel fiber orientations. We normalized all ODFs by the maximum ODF length within each voxel, and calculated fractional anisotropy (FA) from orientation vectors by fitting the data to the usual tensor model.

One of the advantages of the DSI method compared to other high-angular diffusion imaging techniques is the use of multiple b -values. “Optimal” b -value makes sense only if good prior information on the tissue is provided, and if the tissue is fairly uniform in terms of diffusion properties. We aimed to see whole-brain developmental changes in the cat, that is, including both the white and gray matter, such that it would be reasonable to use multiple b -values. The use of multiple b -values is still effective even after we extract only the second moment of the PDF.

Aliasing in PDF could potentially result from not sampling finely enough in q -space. This aliasing would bias the PDF and reconstructed fibers in coordinate directions. However, we do not believe this was a problem in our imaging, because (a) we sampled 515 points in q -space, and (b) we did not observe bias of reconstructed fibers in coordinate directions.

Diffusion data analyses—tractography

We used a streamline algorithm for diffusion tractography (Wedeen et al., 1995; Mori et al., 1999; Wedeen et al., 2008). Trajectories were propagated by always pursuing the orientation vector of least curvature. Thalamo-cortical tracts to the visual cortex were determined as fibers passing through both seed regions placed in the visual cortex and in the middle of the body of the tracts. Cortico-cortical tracts in the temporal lobe were detected using seed regions placed in the middle of the body of the tracts. The cingulum bundle and superior longitudinal fasciculus (SLF) were first detected using a coronal slice filter placed in the middle of the brain, which enabled us to find pathways going through the slice. We further eliminated the other pathways for visualization purposes by using other seed regions close to the slice filter. These procedures allowed us to identify pathways going through both the slice filter and the seed regions.

We terminated tracking when the angle between two consecutive orientation vectors was greater than the given threshold (35°), or when the fibers extended outside of the brain surface, by using mask images of the brains created by MRICro (<http://www.sph.sc.edu/comd/rorden/mricro.html>) for each specimen. In many tractography studies, FA values are used to terminate fibers in the gray matter, which in adults has lower FA values than the white matter. However, as one of the objectives of our study was to detect fibers in low FA areas, we instead used brain mask volumes to terminate tractography fibers. Trajectories were displayed on a 3D workstation (TrackVis, <http://trackvis.org>). The color-coding of fibers is based on a standard RGB code, applied to the vector between the end-points of each fiber (Schmahmann et al., 2007). For Fig. 6, we projected the terminal areas of the thalamo-cortical tracts (up to 4 mm depth from the brain surface) onto the brain surface using MRICro. For Fig. 7, we set a sagittal slice filter at the center of the brain to depict callosal connections. For Fig. 8, in addition to the left thalamo-cortical tracts, we placed starting areas of tractography around the secondary visual areas in the right hemisphere in the P35 and P100 brains (Figs. 7B and C), while we placed starting areas around the corpus callosal area in the P0 brain (Fig. 7A) because the callosal connections in the P0 brain were physically disconnected during preparation processes.

Histology—Luxol Fast Blue (for myelinated fibers) counterstained with cresyl violet (for cell bodies)

After MRI scanning, brains were soaked in sucrose solutions (10% and then 30%), frozen and sectioned at $40\ \mu\text{m}$. After a de-fat step, in which the slides were soaked in 1:1 alcohol/chloroform for a few hours and then rehydrated with 95% ethyl alcohol, they were left in luxol fast blue solution in a $56\ ^\circ\text{C}$ oven overnight (14 h). After a rinse with 95% ethyl alcohol and distilled water to remove excess stain, the slides were differentiated in lithium carbonate solution for 30 s, and then in 70% ethyl alcohol for 30 s. The slides were then rinsed in

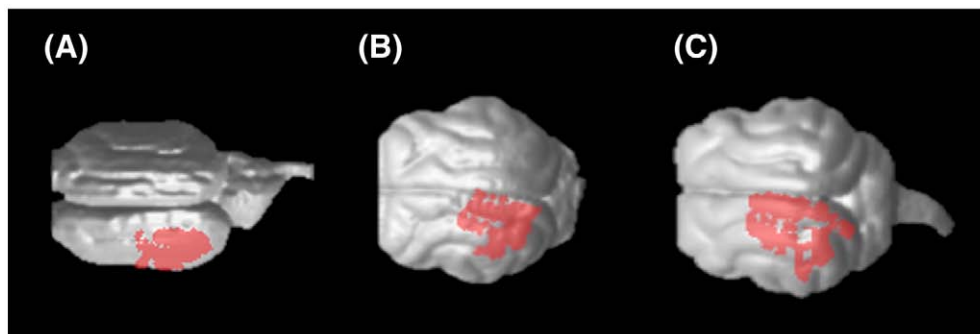


Fig. 6. Terminal areas of the left thalamo-cortical tracts in P0 (A), P35 (B), and P100 (C) brains, superimposed on 3-dimensional brain surface. The left side of the image represents the anterior side of the brain.

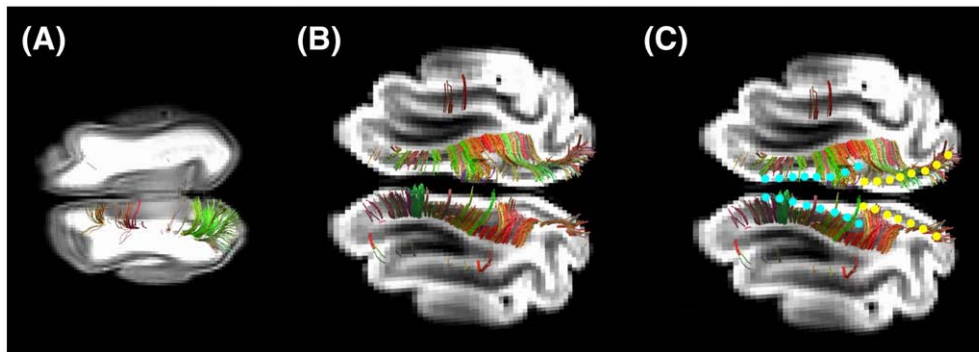


Fig. 7. Callosal connections in the P0 (A) and P100 (B, C) brains superimposed on an axial DWI slice. (C) Borders of areas 17/18 are shown in light blue, while borders of areas 18/19 are shown in yellow. The left side of the image represents the anterior side of the brain.

distilled water, and checked under a microscope to determine that the gray matter was clear and white matter sharply defined in the P100 brain, because there is abundant literature that shows myelination is significantly progressed at P100. We used the same procedure for the P0 and P35 brains. Next, the slides were counterstained in cresyl violet solution for 30–40 s. After a rinse in distilled water, the slides were differentiated in 95% ethyl alcohol for 5 min, in 100% alcohol 2×5 min, and finally in Xylene 2×5 min, and mounted with resinous medium. As a result of these staining procedures, myelinated fibers are stained blue, and neuronal cell bodies are stained pink to violet.

Results

Fractional anisotropy

The P0 brains (Fig. 1A) showed diffuse low FA throughout the white matter, with minimal regional variation except in areas of tightly packed axons such as in the corpus callosum and internal capsule. As development continued (P35, Fig. 1B), LFB stains detected white matter in the deep white matter, primarily involving major projection systems such as the primary visual and sensory motor systems. In these regions, FA was highest and increasing FA was also noted in the surrounding white matter. When more mature (P100, Fig. 1C), myelin is detected throughout the white matter on LFB with associated higher FA values, but similar regional variations persist with the highest FA values centrally in the white matter and lower FA values in the subcortical regions.

Luxol Fast Blue staining

The P0 brain did not show the blue stain for myelin in the white matter using luxol fast blue (Fig. 1D), whereas the P35 brain stained weakly (Fig. 1E), and the P100 brain stained strongly (Fig. 1F). This tendency for the white matter to stain more intensely with advancing

age was consistent across multiple sections and compatible with the changes seen in the FA values (Figs. 1A–C).

Orientation distribution functions

We scanned the neonatal brains a second time, this time with the 9.4T scanner, to obtain higher-resolution images of the fiber tracts in the small P0 brain. The orientation distribution functions (ODFs) (Fig. 2A) successfully revealed multiple local maxima in each voxel in the P0 brain white matter (Fig. 2B), where we had found lower FA values and less myelin than in the later developmental stages.

In the cortical plate of newborn kittens, up to 1 mm in depth, ODFs were single-peaked and mainly oriented orthogonally to the brain surface, which likely corresponding to the cortical plate (e.g. Zhang et al., 2003; Huang et al., 2008). On the surface, there were some multi-peak ODFs, due to artifact. Beyond than 1 mm from the surface, ODFs mainly showed multiple peaks up to the deep white matter, likely corresponding to crossing fibers in the subplate and white matter/intermediate zone.

DSI tractography

We performed DSI tractography and successfully imaged fiber pathways in immature white matter containing low FA values (Fig. 2C). We detected thalamo-cortical tracts between the lateral geniculate nucleus and the primary visual cortex at all ages (Fig. 3). The complexity of tract branching was greater in the P35 and P100 brains compared to the P0 brain. Thus, the main body of the tract was smoother and the fibers beneath the gyri that branched from the body were almost straight in the P0 brain (Fig. 3A), while at later stages of development, fibers in the deep white matter became more branched as they extended into the gyri (Figs. 3B and C). These changes occurred in the cat brain during the first month after birth. Fig. 4 shows the thalamo-cortical tracts on some sequential coronal DWIs,

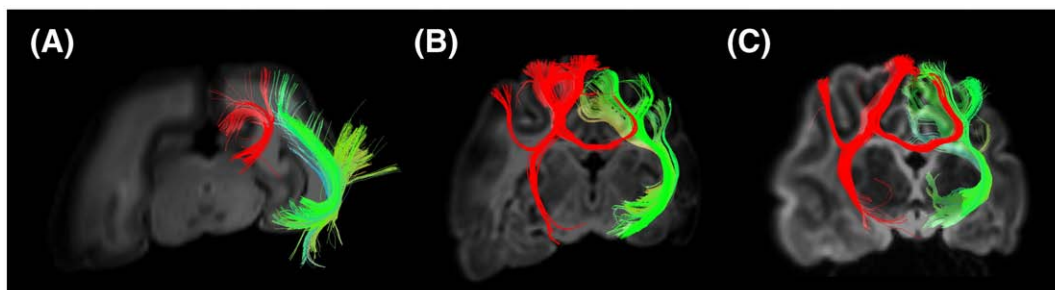


Fig. 8. Oblique coronal views of examples of callosal connections (red) in P0 (A), P35 (B), and P100 (C) brains, in relation with the thalamo-cortical tracts.

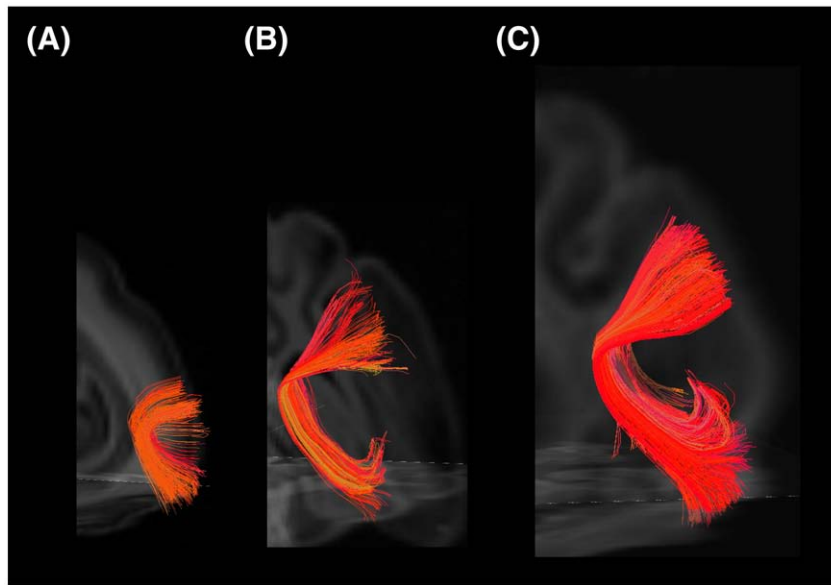


Fig. 9. 3D views of the cortico-cortical tract in the temporal lobe, between the primary auditory cortex and the inferior temporal cortex, in P0 (A), P35 (B), and P100 (C) brains. The left side of the image represents the left side of the brain.

from posterior (A) to anterior (D). Fibers in the deep white matter were found continuously to the brain surface.

To show the effect of the use of the brain mask for terminating tractography, we performed tractography using conventional cut off FA values along with the brain mask, and compared the results those derived only by using a brain mask (Fig. 5). Using a conventional FA mask ($FA > 0.2$), pathways tended to terminate before they entered to the cortical plate (Fig. 5B) compared to those generated by using the brain mask (Fig. 5A).

Fig. 6 shows terminal points of the thalamo-cortical tracts superimposed on sequential axial slices. Both in adult and newborn animals, the terminal areas were located in the lateral gyrus and suprasylvian gyrus (17, 18, 19, 21a, 7, LS (lateral suprasylvian) areas), which well agrees with literature (Jones 2007). We also studied how terminal points of the callosal connections were distributed in the cortex. We found that they appeared to be terminated in the 17/18

border and 18/19 border areas in the young adult (P100) cat (Figs. 7B, C), which has been reported in previous studies (Olavarria and Van Sluyters, 1995). In the earlier stages of development, the distribution of the terminal areas was less specific (Figs. 7A and 8), which supports the theory of exuberant connectivity (Innocenti and Frost, 1979).

Association pathways were also detected (Figs. 9 and 10). Cortico-cortical tracts in the temporal lobe, between the primary auditory cortex and the inferior temporal cortex, were detected at all ages: they were smooth in the P0 brain (Fig. 9A) and took on a sharper angle in the later stages of development (Figs. 9B and C). The cingulum bundle and superior longitudinal fasciculus (SLF) were weakly detected in the P0 brain (Fig. 10A), but became more visible with time (Figs. 10B and C). Although, compared to the P100 brain, the whole length of the SLF was not detected in the P35 brain (Fig. 10B), the cingulum bundle in the P35 brain already showed mature features (Fig. 10E) as the P100 brain (Fig. 10F).

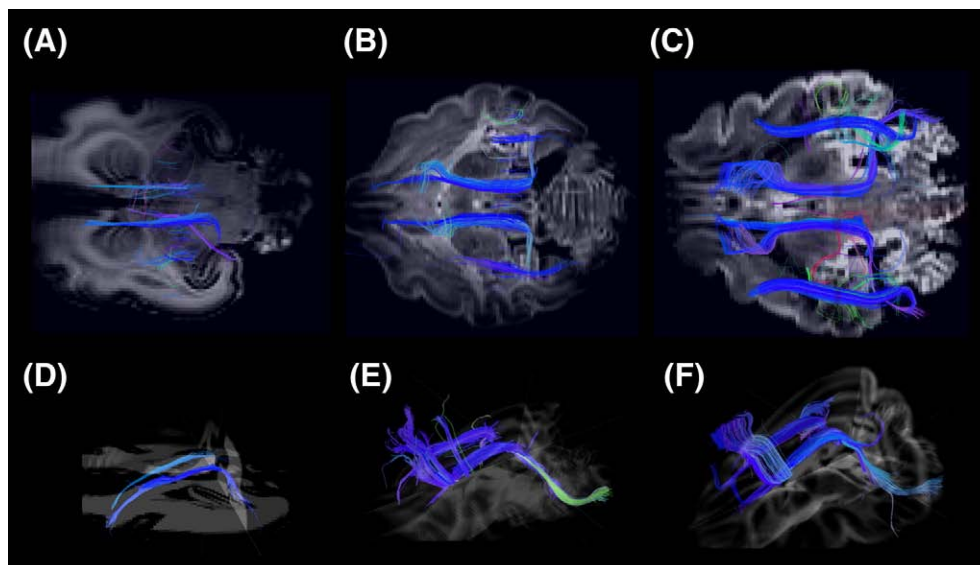


Fig. 10. 3D views of the cingulum bundle and superior longitudinal fasciculus in axial views in P0 (A, D), P35 (B, E), and P100 (C, F) brains. The cingulum bundles are shown separately from oblique angles (D–F). The left side of the image represents the anterior side of the brain.

Discussion

We successfully identified a thalamo-cortical tract and cortico-cortical association pathways in newborn cat brains, overcoming the limitation imposed by crossing fibers in the subplate (SP) and other areas with low FA values. We also observed structural changes in the thalamo-cortical tracts. Whereas the main body of the tract was smoother in newborns, and the fibers branching from it almost straight, at later stages of development, the complexity of the tract increased and the branching fibers curved in parallel with the formation of gyral structures. We further observed structural changes in association fiber pathways. These changes occurred especially during the first month after birth.

One of the strengths of our current study is the demonstration of accurate imaging of the 3-dimensional structure of the white matter pathways. We believe that, significantly, this is the first study to depict 3-dimensional brain structures including the cortex with this level of precision, which may contribute to more thorough understanding of the development of branching of the thalamo-cortical pathways and relation to gyral formation in future studies.

Changes of FA values in the cortex during development

As the mammalian cerebral cortex develops, thalamic axons grow into the immature cortex (cortical plate, CP) and select appropriate cortical targets (Ghosh and Shatz, 1992). The CP, which later develops into the adult cortex, begins to form around prenatal week (W) 20 in humans (Kostovic and Jovanov-Milosevic, 2006). This stage corresponds to embryonic day (E) 20 in cats (Luskin and Shatz, 1985). An initial event in the establishment of the permanent, sensory-driven circuitry is the formation of thalamo-cortical synaptic contacts in the CP; other major afferent fibers, such as the basal-forebrain and cortico-cortical fibers, also grow and accumulate below the CP at E28 to E45 in cats (Issa et al., 1999), and at W22 to W26 in humans. In cats, horizontal connections in the cortex begin developing just after birth, thus reducing the directional coherency in the radial orientation (Callaway and Katz, 1990). In MR imaging studies, a reduction in FA values in the cortex is explained by these sequential events, which were corroborated by the results of our study in cats that showed significantly reduced FA values in the cortex after birth. The corresponding developmental stage for horizontal connections in the human cortex is around W26 to W35, and FA values in the cortex have been reported to be reduced both during and after this stage (McKinstry et al., 2002).

Changes of FA values in the white matter during development

Diffusion studies on developing animal (Zhang et al., 2003, 2005; Huang et al., 2006; Kroenke et al., 2007; Huang et al., 2008; D'Arceuil et al., 2008; Kuo et al., 2008; Baloch et al., 2009), fetal and newborn human brains (Rutherford et al., 1991; Sakuma et al., 1991; Huppi et al., 1998; Neil et al., 1998; Baratti et al., 1999; for review Neil et al., 2002; Prayer et al., 2006; Huang et al., 2009) have reported that FA values increase in the white matter with age. Some investigators have performed diffusion tractography in animals (Zhang et al., 2003; Kim et al., 2003; D'Arceuil et al., 2008) and humans (Bui et al., 2006; Huang et al., 2006; Kasprian et al., 2008; Huang et al., 2009) showing the development of major white matter pathways during myelination.

In the present study, we stained white matter myelin with luxol fast blue. There was strong staining in the P100 brains and relatively weak staining in the P35 brains; no myelin staining was seen in the P0 brains. Although brain white matter myelination is a long process that starts before birth and continues until adulthood, with myelination of the primary motor and sensory tracts visible earlier than that of the cortico-cortical association fibers

(Flechsig, 1920; Yakovlev and Lecours, 1967; Brody et al., 1987), most parts of the human brain show an increase in FA values (approximating adult values) by 2 years of age (Schmithorst et al., 2002). The onset of visible myelination in the brain varies in different fiber tracts and species, but on average, it starts around E40 in the spinal cord and around P20 in the callosal areas in cats (Remahl and Hildebrand, 1982, 1990); therefore, it is likely that myelination occurs in the thalamo-cortical tracts sometime between these periods in cats. This presumed timeframe for myelination would agree with our FA mapping results, which showed gradual increase in FA values in the white matter during development (Figs. 1A–C) and histology (Figs. 1D–F). It would therefore be reasonable to conclude that DSI tractography successfully imaged the entire length of the thalamo-cortical tracts, which had less myelin than those in adult animals.

Significance of the use of DSI tractography for the study of developing brains

The conventional methods that have been used for most developmental axonal tracing histological and MRI studies are associated with three major technical difficulties (Mori, 2007). First, because the white matter appears homogenous in conventional MRI, it is difficult to appreciate intrinsic features of the white matter anatomy. Second, invasive tracer approaches can study only a few white matter tracts at a time and cannot be used for global anatomical characterization, nor can they be used sequentially in the same animal to follow development or the effect of an experiment. Third, the very nature of invasive approaches means that they cannot be applied to examine the human brain *in vivo*. Unlike these methods, diffusion tractography permits examination (1) of white matter axonal connections running in many directions, (2) throughout the whole brain, (3) *in vivo*, and sequentially during growth, learning, and development.

The visualization of the true complexity of a structure would be crucial for understanding functionally important trajectories, because they could be accurately revealed only when we visualize a complex entire structure. To identify functionally important connectivity from among all of the anatomical pathways detected, it will be important for future studies to combine *in vivo* tractography and functional connectivity, as is becoming widely used; however, *in vivo* DSI tractography will require significant shortening of the image acquisition time.

Although the acquisition time used in this study is not applicable for *in vivo* study, we could take a DSI scan, for example in less than 1 h, depending on the pre-set spatial resolution we choose, and how much averaging we do. The final resolution for tractography may depend largely on the spatial resolution and on SNR, which relies in part on the number of averaging steps done. Currently, typical spatial resolution for a standard 1-h DSI scan to obtain decent tractography results of a human brain is about 3 mm. However, the outcomes of scanning with such SNR and spatial resolution are not comparable to those obtained in this study.

Several potential solutions may help to shorten DSI acquisition time. First, since DSI samples symmetrically across the *q*-space, we can sample one of the two hemispheres (or one of the two directions across the *q*-space). If we acquire only half the data, and so reduce our standard DSI of 515 samples to just 258, we henceforth reduce the scan time in half. Recently, Kuo et al. (2008) compared standard and 203 DSI samplings, and reported that the 203 samplings might be comparable to the 515 samplings, with certain maximum *b*-value, resulting in similar field of view in the PDF domain. We hope to shorten the DSI scan times by continuing such kinds of effort and expect that we will be able to perform fine *in vivo* DSI tractography with results comparable to those acquired with *ex vivo* imaging.

Limitations of the current tractography techniques

In infant or even fetal brains, the SP is characterized by very low FA values and the adjacent cortex clearly shows higher FA values than the SP (highly anisotropic until W32 in humans, for review see Prayer et al. 2006). However, whether and in what extent this phenomenon is related to the columnar architecture of the developing CP and the existence of unmyelinated intracortical fibers is still debatable. In this study, we showed the orthogonal course of fibers into the CP (Figs. 4 and 5) and claimed that these trajectories are the result of real axonal connections, but we admit that there is still the possibility that they are only an artificial consequence of the local columnar cellular cortical organization.

Although we mainly attributed the low FA values of the SP area in this study to the high amount of crossing fibers of the SP, because our findings that ODFs mainly showed multiple peaks up to the deep white matter (beyond than 1 mm from the surface) are likely corresponding to crossing fibers in the SP and white matter/intermediate zone. However, this claim may not be entirely correct, since the SP also shows a high amount of non-axonal cellular or molecular components, which may also influence the local diffusion properties and lead to local anisotropy visualized as trajectory (see Kostovic and Jovanov-Milosevic, 2006). Detailed correlation studies with histology will help in a better interpretation of diffusion tractography results in this developmental stage.

The increased sensitivity of the technique used in this study in low FA regions may be a disadvantage in high FA regions (maybe in overestimating the local fiber architecture by including (glial) cellular elements). However, in very high FA regions, ODFs tend to be like ellipsoid obtained from DTI, so the possible disadvantage in those regions seem to be less problematic.

In this study, we used a threshold of 35° for tractography. Although angle thresholds to terminate tractography fibers are arbitrary chosen in many tractography studies (ranging about 35°–60°), such arbitrary selection may cause erroneous findings of pathways. According to the complexity of the visualized fibers and the fact that the regional differences in the maturation of the gray matter (e.g. thickness and contents of the SP/CP) and the white matter (e.g. degrees of myelination, cell migration) depend on developmental stages, we would have to think in future studies about different tractography settings for different brain areas in different developmental stages. We also would have to think about different settings for different species because the final brain size and gyral patterns are very different across species. For example, adult rat or mouse brains are very similar to those of newborn kittens and fetal human brains in early stages. Also, optimal angle threshold of each brain area may depend on spatial resolutions that are partly dependent on the brain sizes.

Acknowledgments

We greatly appreciate Nichole Eusemann for her helpful editorial comments. This work was supported by NIH (RO1 MH 64044), the National Science Foundation PHY 0855161, PHY 0855453 and the Ellison Medical Foundation #208556.

References

- Allendoerfer, K.L., Shatz, C.J., 1994. The subplate, a transient neocortical structure: its role in the development of connections between thalamus and cortex. *Ann. Rev. Neurosci.* 17, 185–218.
- Baloch, S., Verma, R., Huang, H., Khurd, P., Clark, S., Yarowsky, P., Abel, T., Mori, S., Davatzikos, C., 2009. Quantification of brain maturation and growth patterns in C57BL/6j mice via computational neuroanatomy of diffusion tensor imaging. *Cerebr. Cortex* 19, 675–687.
- Baratti, C., Barnett, A.S., Pierpaoli, C., 1999. Comparative MR imaging study of brain maturation in kittens with T1, T2, and the trace of the diffusion tensor. *Radiology* 210, 133–142.
- Barkovich, A.J., Kjos, B.O., Jackson, D.E., Norman, D., 1988. Normal maturation of the neonatal and infant brain: MR imaging at 1.5 T. *Radiology* 166, 173–180.
- Basser, P.J., Mattiello, J., LeBihan, D., 1994. Estimation of the effective self-diffusion tensor from the NMR spin echo. *J. Magn. Reson. B* 103, 247–254.
- Basser, P.J., Pajevic, S., Pierpaoli, C., Duda, J., Aldroubi, A., 2000. *In vivo* fiber tractography using DT-MRI data. *Magn. Reson. Med.* 44, 625–632.
- Bassi, L., Ricci, D., Volzone, A., Allsop, J.M., Srinivasan, L., Pai, A., Ribes, C., Ramenghi, L.A., Mercuri, E., Mosca, F., Edwards, A.D., Cowan, F.M., Rutherford, M.A., Counsell, S.J., 2008. Probabilistic diffusion tractography of the optic radiations and visual function in preterm infants at term equivalent age. *Brain* 131, 573–582.
- Beaulieu, C., Allen, P.S., 1994. Determinants of anisotropic water diffusion in nerves. *Magn. Reson. Med.* 31, 394–400.
- Berman, J.I., Mukherjee, P., Partridge, S.C., Miller, S.P., Ferriero, D.M., Barkovich, A.J., Vigneron, D.B., Henry, R.G., 2005. Quantitative diffusion tensor MRI fiber tractography of sensorimotor white matter development in premature infants. *NeuroImage* 27, 862–871.
- Brody, B.A., Kinney, H.C., Kloman, A.S., Gilles, F.H., 1987. Sequence of central nervous system myelination in human infancy. I. An autopsy study of myelination. *J. Neuropathol. Exp. Neurol.* 46, 28–301.
- Bui, T., Daire, J.-L., Chalard, F., Zaccaria, I., Alberti, C., Elmaleh, M., Garel, C., Luton, D., Blanc, N., Sebag, G., 2006. Microstructural development of human brain assessed in utero by diffusion tensor imaging. *Pediatr. Radiol.* 36, 1133–1140.
- Callaway, E.M., Katz, L.C., 1990. Emergence and refinement of clustered horizontal connections in cat striate cortex. *J. Neurosci.* 10, 1134–1153.
- Catani, M., Howard, R.J., Pajevic, S., Jones, D.K., 2002. Virtual *in vivo* interactive dissection of white matter fasciculi in the human brain. *NeuroImage* 17, 77–94.
- Cellerini, M., Konze, A., Caracchini, G., Santoni, M., Dal Pozzo, G., 1997. Magnetic resonance imaging of cerebral associative white matter bundles employing fast-scan techniques. *Acta Anat. (Basel)* 158, 215–221.
- Conturo, T.E., Lori, N.F., Cull, T.S., Akbudak, E., Snyder, A.Z., Shimony, J.S., McKinstry, R.C., Burton, H., Raichle, M.E., 1999. Tracking neuronal fiber pathways in the living human brain. *Proc. Natl. Acad. Sci. U. S. A.* 96, 10422–10427.
- D'Arceuil, H., Liu, C., Levitt, P., Thompson, B., Kosofsky, B., de Crespigny, A., 2008. Three-dimensional high-resolution diffusion tensor imaging and tractography of the developing rabbit brain. *Dev. Neurosci.* 30, 262–275.
- Dubois, J., Hertz-Pannier, L., Dehaene-Lambertz, G., Cointepas, Y., Le Bihan, D., 2006. Assessment of the early organization and maturation of infants' cerebral white matter fiber bundles: a feasibility study using quantitative diffusion tensor imaging and tractography. *NeuroImage* 30, 1121–1132.
- Dubois, J., Dehaene-Lambertz, G., Perrin, M., Mangin, J.-F., Cointepas, Y., Duchesnay, E., Le Bihan, D., Hertz-Pannier, L., 2008a. Asynchrony of the early maturation of white matter bundles in healthy infants: Quantitative landmarks revealed noninvasively by diffusion tensor imaging. *Hum. Brain Mapp.* 29, 14–27.
- Dubois, J., Dehaene-Lambertz, G., Soares, C., Cointepas, Y., Le Bihan, D., Hertz-Pannier, L., 2008b. Microstructural correlates of infant functional development: Examples of the visual pathways. *J. Neurosci.* 28, 1943–1948.
- Flechsig, P., 1920. *Anatomie des menschlichen Gehirns und Rückenmarks auf myelogenetischer Grundlage*. Thieme, Leipzig.
- Ghosh, A., Shatz, C.J., 1992. Pathfinding and target selection by developing geniculocortical axons. *J. Neurosci.* 12, 39–55.
- Hagmann, P., Cammoun, L., Gigandet, X., Meuli, R., Honey, C.J., Wedeen, V.J., Sporns, O., 2008. Mapping the structural core of human cerebral cortex. *PLoS Biol.* 6, e159.
- Hermann, K., Antonini, A., Shatz, C.J., 1994. Ultrastructural evidence for synaptic interactions between thalamocortical axons and subplate neurons. *Eur. J. Neurosci.* 6, 1729–1742.
- Huang, H., Zhang, J., Wakana, S., Zhang, W., Ren, T., Richards, L., Yarowsky, P., Donohue, P., Graham, E., van Zijl, P.C.M., Mori, S., 2006. White and gray matter development in human fetal, newborn and pediatric brains. *NeuroImage* 33, 27–38.
- Huang, H., Akira, Yamamoto, Hossain, M.A., Younes, L., Mori, S., 2008. Quantitative cortical mapping of fractional anisotropy in developing rat brains. *J. Neurosci.* 28, 1427–1433.
- Huang, H., Xue, R., Zhang, J., Ren, T., Richards, L., Yarowsky, P., Miller, M.I., Mori, S., 2009. Anatomical characterization of human fetal brain development with diffusion tensor magnetic resonance imaging. *J. Neurosci.* 29, 4263–4273.
- Huppi, P.S., Maier, S.E., Peled, S., Zientara, G.P., Barnes, P.D., Jolesz, F.A., Volpe, J.J., 1998. Microstructural development of human newborn cerebral white matter assessed *in vivo* by diffusion tensor magnetic resonance imaging. *Pediatr. Res.* 44, 584–590.
- Innocenti, G.M., Frost, D.O., 1979. Effects of visual experience on the maturation of the efferent system to the corpus callosum. *Nature* 280, 231–234.
- Issa, N.P., Trachtenberg, J.T., Chapman, B., Zahs, K.R., Stryker, M.P., 1999. The critical period for ocular dominance plasticity in the ferret's visual cortex. *J. Neurosci.* 19, 6965–6978.
- Jones, E.G., 2007. *The thalamus*. Cambridge University Press, NY.
- Jones, D.K., Simmons, A., Williams, S.C., Horsfield, M.A., 1999. Non-invasive assessment of axonal fiber connectivity in the human brain via diffusion tensor MRI. *Magn. Reson. Med.* 42, 37–41.
- Johnson, J.K., Casagrande, V.A., 1993. Prenatal development of axon outgrowth and connectivity in the ferret visual system. *Vis. Neurosci.* 10, 117–130.
- Kasprian, G., Brugger, P.C., Weber, M., Krssak, M., Krampfl, E., Herold, C., Prayer, D., 2008. *In utero* tractography of fetal white matter development. *NeuroImage* 43, 213–224.
- Kim, D.S., Kim, M., Ronen, I., Formisano, E., Kim, K.H., Ugurbil, K., Mori, S., Goebel, R., 2003. *In vivo* mapping of functional domains and axonal connectivity in cat visual cortex using magnetic resonance imaging. *Magn. Reson. Imaging* 21, 1131–1140.
- Kostovic, I., Rakic, P., 1990. Developmental history of the transient subplate zone in the visual and somatosensory cortex of the macaque monkey and human brain. *J. Comput. Neurol.* 297, 441–470.
- Kostovic, I., Jovanov-Milosevic, N., 2006. The development of cerebral connections during the first 20–45 weeks' gestation. *Semin. Fetal Neonatal Med.* 11, 415–422.

- Kroenke, C.D., Van Essen, D.C., Inder, T.E., Rees, S., Bretthorst, G.L., Neil, J.J., 2007. Microstructural changes of the baboon cerebral cortex during gestational development reflected in magnetic resonance imaging diffusion anisotropy. *J. Neurosci.* 27, 12506–12515.
- Kuo, L.-W., Chen, J.-H., Wedeen, V.J., Tseng, W.Y., 2008. Optimization of diffusion spectrum imaging and q-ball imaging on clinical MRI system. *NeuroImage* 41, 7–18.
- Le Bihan, D., Mangin, J.F., Poupon, C., Clark, C.A., Pappata, S., Molko, N., Chabriat, H., 2001. Diffusion tensor imaging: concepts and applications. *J. Magn. Reson. Imaging* 13, 534–546.
- Lin, C.P., Wedeen, V.J., Chen, J.H., Yao, C., Tseng, W.Y., 2003. Validation of diffusion spectrum magnetic resonance imaging with manganese-enhanced rat optic tracts and *ex vivo* phantoms. *NeuroImage* 19, 482–495.
- Luskin, M.B., Shatz, C.J., 1985. Neurogenesis of the cat's primary visual cortex. *J. Comp. Neurol.* 242, 611–631.
- Maas, L.C., Mukherjee, P., Carballido-Gamio, J., et al., 2004. Early laminar organization of the human cerebrum demonstrated with diffusion tensor imaging in extremely premature infants. *NeuroImage* 22, 1134–1140.
- Makris, N., Worth, A.J., Sorensen, A.G., Papadimitriou, G.M., Wu, O., Reese, T.G., Wedeen, V.J., Davis, T.L., Stakes, J.W., Caviness, V.S., Kaplan, E., Rosen, B.R., Pandya, D.N., Kennedy, D.N., 1997. Morphometry of *in vivo* human white matter association pathways with diffusion-weighted magnetic resonance imaging. *Ann. Neurol.* 42, 951–962.
- McKinstry, R.C., Mathur, A., Miller, J.H., Ozcan, A., Snyder, A.Z., Schefft, G.L., Almli, C.R., Shiran, S.I., Conturo, T.E., Neil, J.J., 2002. Radial organization of developing preterm human cerebral cortex revealed by non-invasive water diffusion anisotropy MRI. *Cereb. Cortex* 12, 1237–1243.
- Mori, S., 2007. Introduction to Diffusion Tensor Imaging 1st Edition. Elsevier Science.
- Mori, S., Crain, B.J., Chacko, V.P., van Zijl, P.C., 1999. Three-dimensional tracking of axonal projections in the brain by magnetic resonance imaging. *Ann. Neurol.* 45, 265–269.
- Neil, J.J., Shiran, S.I., McKinstry, R.C., Schefft, G.L., Snyder, A.Z., Almli, C.F., Akbudak, E., Aronovitz, J.A., Miller, J.P., Lee, B.C., Conturo, T.E., 1998. Normal brain in human newborns: apparent diffusion coefficient and diffusion anisotropy measured by using diffusion tensor MR imaging. *Radiology* 15, 57–66.
- Neil, J.J., Miller, J., Mukherjee, P., Huppi, P.S., 2002. Diffusion tensor imaging of normal and injured developing human brain—a technical review. *NMR Biomed.* 15, 543–552.
- Olavarría, J.F., Van Sluyters, R.C., 1995. Overall pattern of callosal connections in visual cortex of normal and enucleated cats. *J. Comp. Neurol.* 363, 161–176.
- O'Leary, D.D.M., Schlaggar, B.L., Tuttle, R., 1994. Specification of neocortical areas and thalamocortical connections. *Ann. Rev. Neurosci.* 17, 419–439.
- Partridge, S.C., Mukherjee, P., Henry, R.G., Miller, S.P., Berman, J.I., Jin, H., Lu, Y., Glenn, O.A., Ferriero, D.M., Barkovich, A.J., Vigneron, D.B., 2004. Diffusion tensor imaging: serial quantitation of white matter tract maturity in premature newborns. *NeuroImage* 22, 1302–1314.
- Paus, T., Collins, D.L., Evans, A.C., Leonard, G., Pike, B., Zijdenbos, A., 2001. Maturation of white matter in the human brain: a review of magnetic resonance studies. *Brain Res. Bull.* 54, 255–266.
- Pierpaoli, C., Jezzard, P., Basser, P.J., Barnett, A., Di Chiro, G., 1996. Diffusion tensor MR imaging of the human brain. *Radiology* 201, 637–648.
- Prayer, D., Barkovich, A.J., Kirschner, D.A., Prayer, L.M., Roberts, T.P., Kucharczyk, J., Moseley, M.E., 2001. Visualization of nonstructural changes in early white matter development on diffusion-weighted MR images: evidence supporting premyelination anisotropy. *Am. J. Neuroradiol.* 22, 1572–1576.
- Prayer, D., Kasprian, G., Krampfl, E., Ulm, B., Witzani, L., Prayer, L., Brugger, P.C., 2006. MRI of normal fetal brain development. *Eur. J. Radiol.* 57, 199–216.
- Remahl, S., Hildebrand, C., 1982. Changing relation between onset of myelination and axon diameter range in developing feline white matter. *J. Neurol. Sci.* 54, 33–45.
- Remahl, S., Hildebrand, C., 1990. Relations between axons and oligodendroglial cells during initial myelination. II. The individual axon. *J. Neurocytol.* 19, 883–898.
- Rollins, N.K., 2007. Clinical applications of diffusion tensor imaging and tractography in children. *Pediatr. Radiol.* 37, 769–780.
- Rutherford, M.A., Cowan, F.M., Manzur, A.Y., Dubowitz, L.M., Pennock, J.M., Hajnal, J.V., Young, I.R., Bydder, G.M., 1991. MR imaging of anisotropically restricted diffusion in the brain of neonates and infants. *J. Comput. Assist. Tomogr.* 15, 188–198.
- Sakuma, H., Nomura, Y., Takeda, K., Tagami, T., Nakagawa, T., Tamagawa, Y., Ishii, Y., Tsukamoto, T., 1991. Adult and neonatal human brain: diffusional anisotropy and myelination with diffusion weighted MR imaging. *Radiology* 180, 229–233.
- Schmahmann, J.D., Pandya, D.N., Wang, R., Dai, G., D'Arceuil, H.E., de Crespigny, A.J., Wedeen, V.J., 2007. Association fibre pathways of the brain: parallel observations from diffusion spectrum imaging and autoradiography. *Brain* 130, 630–653.
- Schmithorst, V.J., Wilke, M., Dardzinski, B.J., Holland, S.K., 2002. Correlation of white matter diffusivity and anisotropy with age during childhood and adolescence: a cross-sectional diffusion-tensor MR imaging study. *Radiology* 222, 212–218.
- Takahashi, E., Ohki, K., Kim, D.S., 2007. Diffusion tensor studies dissociated two fronto-temporal pathways in the human memory system. *NeuroImage* 34, 827–838.
- Takahashi, E., Ohki, K., Kim, D.S., 2008. Dissociated pathways for successful memory retrieval from the human parietal cortex: anatomical and functional connectivity analyses. *Cereb. Cortex* 18, 1771–1778.
- Ulfing, N., Neudorfer, F., Bohl, J., 2000. Transient structures of the human fetal brain: subplate, thalamic reticular complex, ganglionic eminence. *Histol. Histopathol.* 15, 771–790.
- Van der Knaap, M.S., Valk, J., 1990. MR imaging of the various stages of normal myelination during the first year of life. *Neuroradiology* 31, 459–470.
- Wedeen, V.J., Davis, T.L., Weisskoff, R.M., Tootell, R., Rosen, B.R., Belliveau, J.W., 1995. White matter connectivity explored by MRI. Proceedings of the First International Conference for Functional Mapping of the Human Brain, Paris; P1.69.
- Wedeen, V.J., Hagmann, P., Tseng, W.Y., Reese, T.G., Weisskoff, R.M., 2005. Mapping complex tissue architecture with diffusion spectrum magnetic resonance imaging. *Magn. Reson. Med.* 54, 1377–1386.
- Wedeen, V.J., Wang, R.P., Schmahmann, J.D., Benner, T., Tseng, W.Y., Dai, G., Pandya, D.N., Hagmann, P., D'Arceuil, H., de Crespigny, A.J., 2008. Diffusion spectrum magnetic resonance imaging (DSI) tractography of crossing fibers. *NeuroImage* 41, 1267–1277.
- Wimberger, D.M., Roberts, T.P., Barkovich, A.J., Prayer, L.M., Moseley, M.E., Kucharczyk, J., 1995. Identification of "premyelination" by diffusion-weighted MRI. *J. Comput. Assist. Tomogr.* 19, 28–33.
- Yakovlev, P.I., Lecours, A.R., 1967. The myelogenetic cycles of regional maturation in the brain. In: Minowski, A (Ed.), *Regional Development of the Brain in Early Life*. Blackwell, Oxford, pp. 3–69.
- Yoo, S.S., Park, H.J., Soul, J.S., Mamata, H., Park, H., Westin, C.F., Bassan, H., Du Plessis, A.J., Robertson, R.L., Maier, S.E., Ringer, S.A., Volpe, J.J., Zientara, G.P., 2005. *In vivo* visualization of white matter fiber tracts of preterm- and term-infant brains with diffusion tensor magnetic resonance imaging. *Invest. Radiol.* 40, 110–115.
- Zhai, G., Lin, W., Wilber, K.P., Gerig, G., Gilmore, J.H., 2003. Comparisons of regional white matter diffusion in healthy neonates and adults performed with a 3.0-T head-only MR imaging unit. *Radiology* 229, 673–681.
- Zhang, J., Richards, L.J., Yarowsky, P., Huang, H., van Zijl, P.C.M., Mori, S., 2003. Three-dimensional anatomical characterization of the developing mouse brain by diffusion tensor microimaging. *NeuroImage* 20, 1639–1648.
- Zhang, J., Chen, Y., Hardwick, J.M., Miller, M.I., Plachez, C., Richards, L.J., Yarowsky, P., van Zijl, P.C.M., Mori, S., 2005. Magnetic resonance diffusion tensor microimaging reveals a role for Bcl-x in brain development and homeostasis. *J. Neurosci.* 25, 1881–1888.